

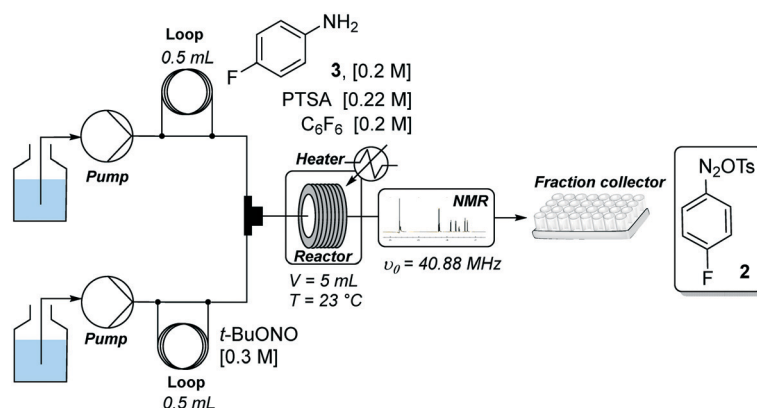


4-fluorobenzene diazonium tosylate **2**. We recently described the palladium-catalyzed direct C–H arylation of indole-3-acetic acid derivatives with arenediazonium salts in a mixture of MeOH–DMF–EtOAc as a solvent.<sup>17</sup> Building on these recent results, we reasoned that 4-fluorobenzene diazonium tosylate **2** should be ideally prepared in MeOH with the subjacent idea of anticipating a prospective diazotization-coupling telescoped process. A few years ago, we validated a two-step telescoped flow process approach involving the diazotization of anilines in MeOH, followed by palladium-catalyzed Heck coupling with methyl acrylate.<sup>18</sup> With these studies in mind, we were relatively confident about succeeding in preparing diazonium salt **2** in MeOH with the two-stream flow device depicted in Scheme 1. The two inlets were equipped with 0.5 mL injection loops. The first loop was loaded with aniline **3** (0.2 M), *p*-toluenesulfonic acid (PTSA, 0.22 M) and C<sub>6</sub>F<sub>6</sub> (0.2 M) in MeOH, while the second loop was filled with a solution of *t*-BuONO (0.3 M) in MeOH. The two streams were mixed in a T-shaped mixer and the resulting mixture was reacted in a PEEK coil reactor (5 mL) maintained at the desired temperature. The outlet of the reactor was connected to the flow cell of a benchtop NMR spectrometer.<sup>19–21</sup> The NMR conversion was determined through 1D <sup>19</sup>F experiments at 40.88 MHz in stop-flow mode. The advantages of monitoring the formation of **2** by <sup>19</sup>F experiments compared to more traditional <sup>1</sup>H experiments is three fold.<sup>22–24</sup> First, the large range of chemical shifts, typically ranging from –300 to 100 ppm, limits unwanted signal overlapping of aromatic protons which is one of the main issues for <sup>1</sup>H experiments conducted on low-field benchtop spectrometers. Second, the <sup>19</sup>F nucleus is 100% naturally abundant, allowing fast measurements with 83% of the <sup>1</sup>H nucleus receptivity. Third, the integrated field-frequency fluorine lock system of the NMR spectrometer allows the use of non-deuterated solvents. Hexafluorobenzene (C<sub>6</sub>F<sub>6</sub>) was used to calibrate the <sup>19</sup>F chemical shifts with fluorine atoms resonating at –164.9 ppm. Note that to optimize data acquisition, a small <sup>19</sup>F spectral width was chosen between –20 and –140 ppm (see Fig. 2 and 3). Such conditions led to controlled folding of the C<sub>6</sub>F<sub>6</sub> <sup>19</sup>F peak at

–164.9 ppm to –39 ppm (see Fig. 2 and 3), which allowed the use of the folded peak as a chemical shift reference. The main limitations of the in-line NMR analysis are those mainly associated with the use of a medium magnetic field that results in a relatively low sensitivity (limit of detection in the mM range for abundant nuclei).

Fig. 2 shows the spectra of crude mixtures recorded in MeOH within 320 seconds (32 scans) corresponding to experiments conducted at a temperature ranging from 30 to 60 °C and within 15 to 30 minutes of residence time. To our surprise, no formation of the diazonium salt **2** could be detected at 30 °C and only a low conversion was observed at 40–45 °C after 30 minutes of residence time. This result was unanticipated since most anilines are usually diazotized within a few minutes under similar flow conditions in MeOH.<sup>18</sup> Increasing the temperature to 60 °C allowed, after only 15 minutes of residence time, a substantial conversion which became complete within 30 minutes as evidenced by the disappearance of the starting anilinium **4** (–115 ppm). Unfortunately, together with the formation of the expected diazonium salt **2** (–85 ppm), we observed the appearance of another singlet at –63 ppm assigned to the unanticipated diazonium salt **5**. The latter was formed by the nucleophilic aromatic substitution of the fluorine atom by methanol followed by counter-anion metathesis. The strong electron-withdrawing properties of the diazonium function strongly activates the aromatic ring toward the nucleophilic attack of MeOH which likely proceeds through a standard addition–elimination mechanism.<sup>25–27</sup> After 60 minutes of residence time at 60 °C, the targeted diazonium salt **2** almost completely disappeared in favor of the unwanted diazonium salt **5**.

Facing these unexpected results, we reasoned that the high lability of the fluorine atom of diazonium salt **2** required the use of a non-nucleophilic solvent as recently demonstrated by Schmidt *et al.*<sup>28</sup> In this frame, we reevaluated our flow process by switching the solvent from MeOH to THF which is known to be a suitable solvent for diazonium salt synthesis (Fig. 3).<sup>29</sup> We ruled out the use of DMF as the solvent since preliminary experiments suggested



Scheme 1 Two-stream flow device for the optimization of the diazonium salt formation.

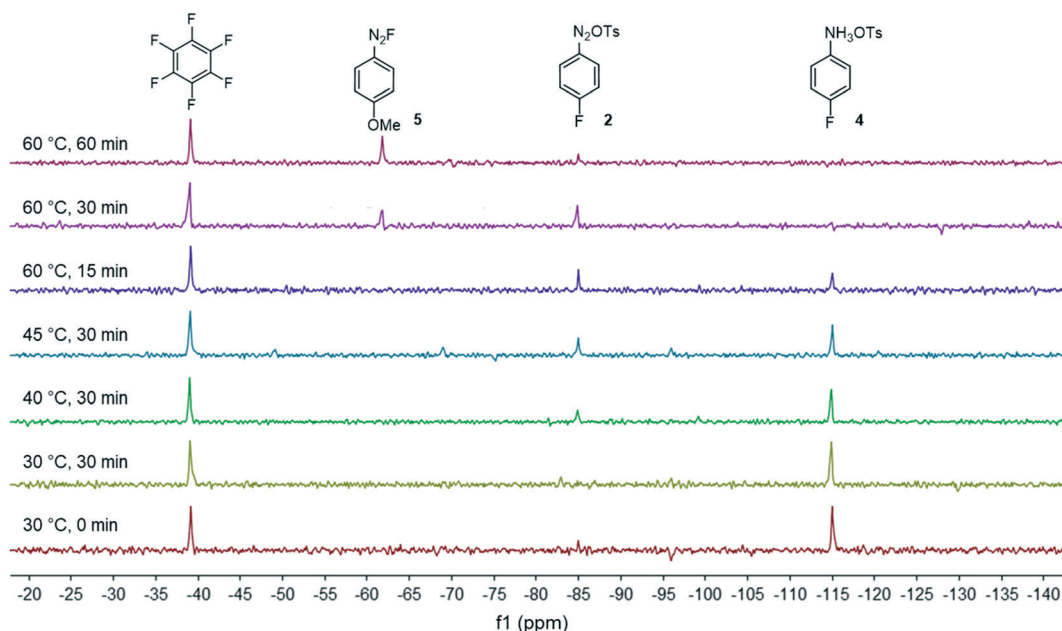


Fig. 2 Monitoring of the diazonium salt formation in MeOH by in-line  $^{19}\text{F}$  NMR analysis at 40.88 MHz.

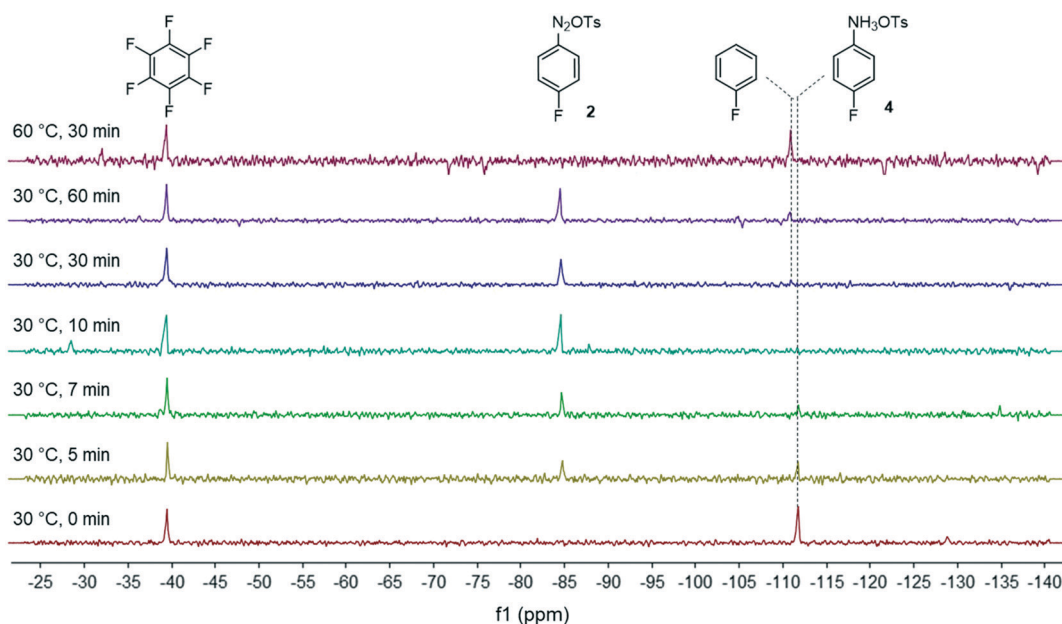


Fig. 3 Monitoring of the diazonium salt formation in THF by in-line  $^{19}\text{F}$  NMR analysis at 40.88 MHz.

that DMF favored the diazonium salt decomposition *via* a dediazotization pathway.<sup>30</sup> We were satisfied to see that in THF, the kinetics of the diazonium formation greatly increased since the starting anilinium **4** was completely consumed after only 10 minutes of residence time. Upon prolonging the residence time (>30 min) or at elevated temperature (60 °C), we observed the progressive degradation of the diazonium salt **2** which underwent a protodiazotisation pathway leading to fluorobenzene.

With the robust flow synthesis of 4-fluorobenzene diazonium tosylate **2** in hand, we continued our studies with

the key direct C–H arylation step. In the first attempt, we transposed the experimental flow conditions we recently used for the coupling of indoles with a variety of diazonium salts,<sup>17</sup> *i.e.*, 44 °C, 74 min residence time and 1.6 equiv. of diazonium, to the coupling of indole **6** with diazonium salt **2** using the two-stream flow setup depicted in Table 1, entry 1. The first injection loop (0.5 mL) was loaded with a solution of 4-fluorobenzene diazonium tosylate **2** in MeOH (0.16 M) which was pumped at  $62.5 \mu\text{L min}^{-1}$  (pump 1) with MeOH as a carrier solvent. A solution of indole **6** (0.1 M), Pd(OAc)<sub>2</sub> (0.01 M) and naphthalene (0.1 M), as the internal standard,

Table 1 Evaluation of the effect of solvents on the reaction outcome

Entry	Solvent 1	Solvent 2	Yield (%) <sup>a</sup> 7/8
1	MeOH	DMF/EtOAc (1/4)	47/2
2	EtOH	DMF/EtOAc (1/4)	10/—
3	<i>i</i> -PrOH	DMF/EtOAc (1/4)	— <sup>b</sup>
4	DMF	DMF/EtOAc (1/4)	5/—
5	MeOH	DMF	44/1
6	MeOH	CH <sub>3</sub> CN	4/<1
7	MeOH/DMF (1/1)	DMF/EtOAc (1/4)	11/0
8	DMF	MeOH/DMF (1/4)	0/0

<sup>a</sup> Yields determined by HPLC. <sup>b</sup> The diazonium salt precipitated in *i*-PrOH.

in a mixture of DMF/EtOAc (1/4, v/v) was loaded in the second injection loop (0.5 mL) and pumped at 62.5  $\mu\text{L min}^{-1}$  (pump 2). Both streams met in a T-shaped piece and the reaction occurred in a stainless steel coil reactor (10 mL, 135  $\mu\text{L min}^{-1}$ ). The crude mixture was collected in a test tube and analyzed by at-line HPLC. Under such experimental conditions, the expected fluorinated indole 7 was formed with a modest yield (47%) and was accompanied by trace amounts, *ca.* 2%, of the undesired arylated indole 8 (Table 1). The latter resulted from the coupling of indole 6 with 4-methoxyphenyl diazonium salt 5 which was formed *in situ* by the nucleophilic aromatic substitution of the fluorine atom with methanol (*vide supra*). With the aim of improving the reaction outcome leading to 7 and eventually suppressing the formation of unwanted indole 8, we explored the possibility of modifying the solvent composition of the reaction media. Regarding the first line delivering the diazonium salt, the substitution of MeOH for EtOH or DMF lowered the reaction yield of indole 7 to only 5–10% (entries 2 and 4), while the use of *i*-PrOH was hampered by the low solubility of diazonium salt 2 (entry 3). We also modified the solvent mixture of the second stream, unfortunately, without success since the substitution of DMF/EtOAc for DMF or CH<sub>3</sub>CN and the decrease of the volume of MeOH were detrimental to the reaction outcome (entries 5–7). Surprisingly, the movement of MeOH from pump 1 to pump 2 completely inhibited the reactivity, suggesting a specific interaction of MeOH with diazonium salt 2 that deserves further clarification (entry 8).

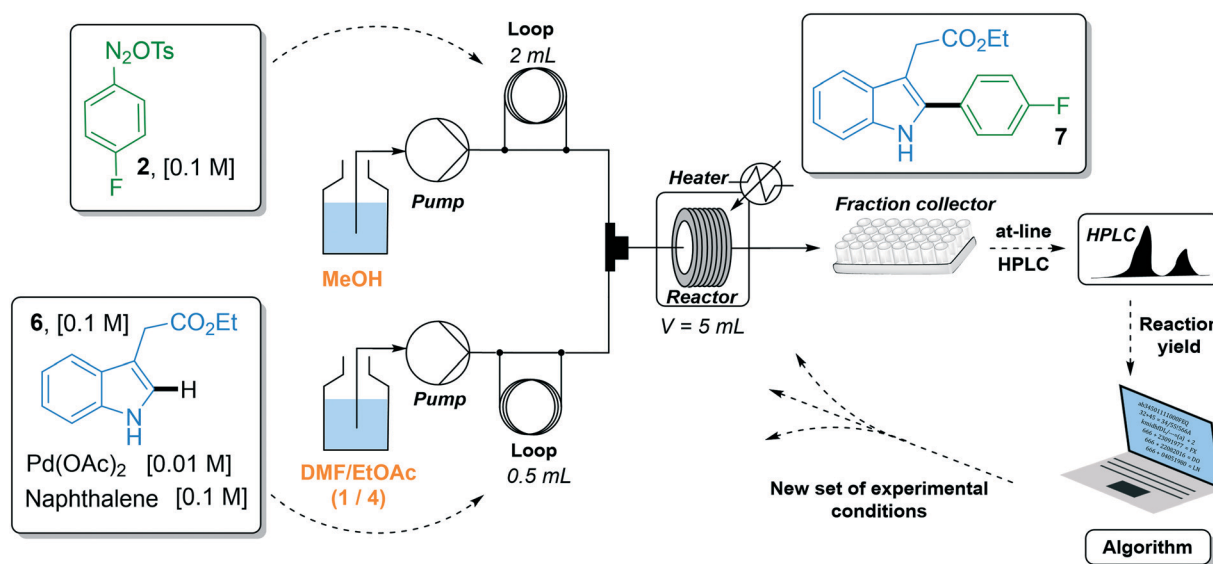
With this short solvent screening, we learned that the combination of solvents initially developed in our previous studies remained the most effective one. The chemical reactivity for the C–H arylation was critically hampered by the absence of MeOH and the stability of 4-fluorobenzene diazonium tosylate 2 was compromised in CH<sub>3</sub>CN or when the content of DMF was increased, likely due to extensive undesired dediazotization pathways.<sup>30</sup> However, the modest reaction yield obtained under the experimental conditions of entry 1 (47%) associated with the long residence time required (74 min) compromised any scaling experiment. Considering that the peculiar reactivity of 4-fluorobenzene diazonium tosylate 2 might not be representative of the other diazonium salts screened in our previous studies,<sup>17</sup> we embarked on a meticulous optimization campaign assisted by an optimization algorithm. Our algorithm-assisted optimization strategy was based on the use of a profoundly modified Nelder–Mead method for which *a priori* and gradient information on the reaction studied was not required since chemical reactions are treated as a black-box. The Nelder–Mead method converts input continuous variables (*e.g.*, temperature, pressure, time, equivalents, *etc.*) into an output variable to be optimized (yield, cost, productivity, *etc.*). The *n*-dimensional chemical space of the objective function is explored through convex polytopes of *n* + 1 vertices, also called simplexes. Each ranked vertex represents an experiment and the algorithm progresses toward an optimum by replacing the worst vertex (experiment) by a new and (always) better vertex. We and

others already demonstrated the suitability of the Nelder–Mead method for chemical problems even in the presence of experimental noise, while traditional gradient-based optimization methods can be severely impacted if experimental failure occurs during the determination of the gradient.<sup>19,31–40</sup> However, the Nelder–Mead method only converges to local optima whose quality highly depends on human-biased initialization and lengthy convergence is generally observed when optimizing large dimensional problems. The modified Nelder–Mead version we used in this study addressed these issues as it i/ offers the possibility of temporarily reducing the dimensionality of the search to speed-up the exploration of a subspace, ii/ associates the Golden search method when the dimensionality reduction leads to 1-D optimizations, iii/ includes either automated or human-assisted mechanisms to escape from unsatisfactory local optima and iv/ uses multiple stopping criteria to limit the total number of experiments.<sup>41</sup>

The C–H arylation of indole **6** with 4-fluorobenzene diazonium tosylate **2** was optimized using the two-stream flow setup depicted in Scheme 2. A solution of 4-fluorobenzene diazonium tosylate **2** in MeOH (0.1 M) was loaded in the first injection loop (2 mL) and flowed at the required flow rate with MeOH as a carrier solvent. A solution of indole **6** (0.1 M), Pd(OAc)<sub>2</sub> (0.01 M) and naphthalene (0.1 M) in a mixture of DMF/EtOAc (1/4, v/v) was loaded in the second injection loop (0.5 mL) and flowed with a mixture of DMF/EtOAc (1/4) at the required flow rate. Both streams met in a T-shaped piece and the reaction occurred in a stainless steel coil reactor (5 mL). The crude mixture was collected in test tubes and analyzed by at-line HPLC. The optimization algorithm was fed with the reaction yield determined by HPLC and a new set of experimental conditions was proposed. In this study, we did not use an automated flow device for two reasons. First, the use of an autonomous

system is fully justified when it can be continuously used without human interception. Yet, we observed that diazonium salt **2** cannot be stored in MeOH at room temperature for more than 4 hours, precluding the use of an autonomous system pumping a mother solution of diazonium **2** in MeOH for several hours. Second, the release of nitrogen gas accompanying the reaction of indole **6** with diazonium **2** complicated the use of an automated online injection in the HPLC system.

The reaction yield was optimized in a four-dimensional space where the residence time, temperature, equivalents of diazonium **2** and loading of palladium catalyst were the four considered input variables  $n$  in the restricted search space of 10–30 min, 25–60 °C, 1–2 equiv. and 1–5 mol%, respectively. The initial starting experiment  $X_0$  was fixed at 10 min of residence time, 25 °C, 1 equiv. of diazonium **2** and 1 mol% Pd(OAc)<sub>2</sub> with  $d$  values of 4 min, 7 °C, 0.2 equiv. and 0.8 mol%, respectively (Fig. 4a and b). Unfortunately, the first simplex, consisting of  $n + 1$  experiments, failed to give the expected arylated indole **7**. In this situation, a specific mechanism included in the optimization algorithm allows the proposal of a new random starting experiment  $X_0$  while keeping the initial fixed  $d$  values. The new  $X_0$  experiment proposed by the machine was 25 min of residence time, 39 °C, 1.7 equiv. of diazonium **2** and 4 mol% Pd(OAc)<sub>2</sub>. With this restart simplex, the reaction yield spectacularly increased, up to 48% in experiment 10. The algorithm further progressed until experiment 18 where it located an optimum (1.7 equiv. diazonium salt, 4.1 mol% Pd, 59 °C and 23 min residence time) corresponding to 80% yield (see Fig. S1 in the ESI†). Being unable to locate a better optimum, the algorithm stopped at experiment 23 after five consecutive rejected simplexes (stopping criterion). The experimental conditions of the 23 experiments can be found in Table S1 in the ESI†. As the optimization was not conducted with an



Scheme 2 Reaction setup for the optimization of indole **6**.

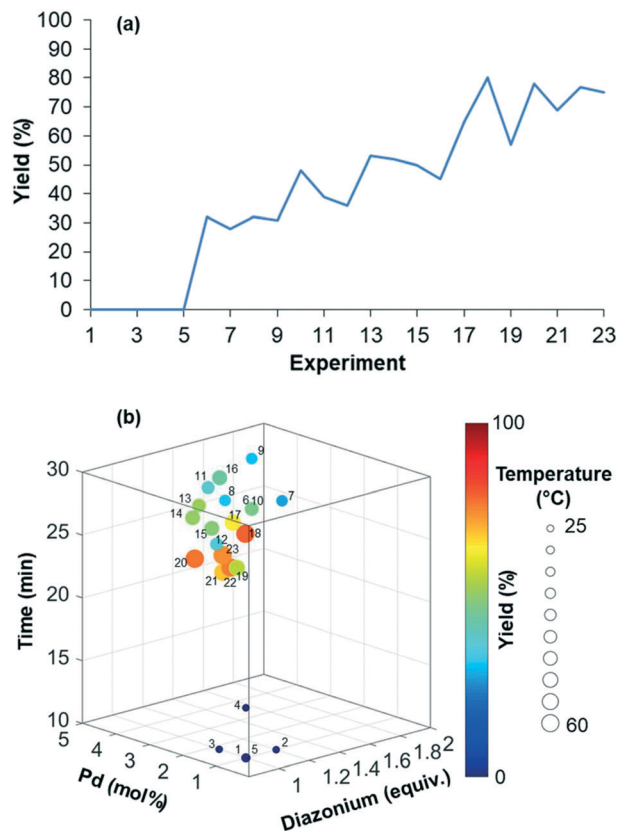


Fig. 4 (a) Maximization of the yield of indole 7. (b) Representation of the four-dimensional experimental conditions for the maximization of the yield of indole 7.

automated flow device, all reactions were conducted twice in order to exclude any potential negative or positive false results. Regarding the random restart simplex proposed by the machine (experiments 6–10), we need to admit that the random simplex proposed inevitably influenced the following experiments. However, as discussed above, the modifications made to our simplex algorithm minimize the impact of human-biased or random initialization on both the rapidity and the quality of the convergence.

In order to install the required dihexylamide group through an amidation step, hydrolysis of the ethyl ester was performed under basic conditions using a two-stream flow setup (Scheme 3a). In the first line, a 1 mL injection loop was loaded with a solution of indole 7 (0.3 M) in THF while in the second line, a solution of 2 M aqueous KOH in MeOH (4/6) was continuously pumped. Both streams met in a T-shaped piece and reacted at 70 °C in a stainless steel coil reactor (5 mL) at a flow rate of 166  $\mu\text{L min}^{-1}$  (30 min residence time). The resulting mixture was collected in vials and purified by flash chromatography to give the corresponding acid 9 with 97% yield. The amidation of acid 9 with dihexylamine was the last step of the synthetic sequence to obtain FGIN-1-27 (1). Amidation is among the most frequently used reactions in medicinal chemistry,<sup>42</sup> and numerous batch procedures and coupling agents have been

developed to address specific needs for mild conditions, reaction rates, efficiency and safety.<sup>43</sup> By contrast, examples of solution-phase amidation in flow are scarce especially because many coupling agents suffer from either a hazardous profile, limited solubility or the formation of by-products which complicate the product isolation.<sup>44–46</sup> For the amidation of acid 9 with dihexylamine, we opted for the combination of 1-ethyl-3-(3-dimethylaminopropyl) carbodiimide hydrochloride (EDC·HCl) with 2-hydroxypyridine oxide (HOPO).<sup>46</sup> This combination is attractive due to their low thermal hazard,<sup>47</sup> fast kinetics and water soluble by-products. A two-stream flow setup was elaborated to proceed with the amidation of acid 9 with dihexylamine (Scheme 3b). In the first stream, a 1 mL injection loop was loaded with a solution of acid 9 (0.23 M), EDC·HCl (0.64 M) and HOPO (0.22 M) in a mixture of THF/H<sub>2</sub>O/acetone (1/2/4) while in the second stream, a 2 mL injection loop was loaded with a solution of dihexylamine (0.25 M) and Et<sub>3</sub>N (1.04 M) in a mixture THF/H<sub>2</sub>O (9/1). Both streams, flowing at 167  $\mu\text{L min}^{-1}$ , met in a T-shaped piece and reacted at 23 °C in a stainless steel coil reactor (10 mL) for a total of 30 min of residence time. The resulting collected mixture was purified by flash chromatography to give FGIN-1-27 (1) with 95% yield.

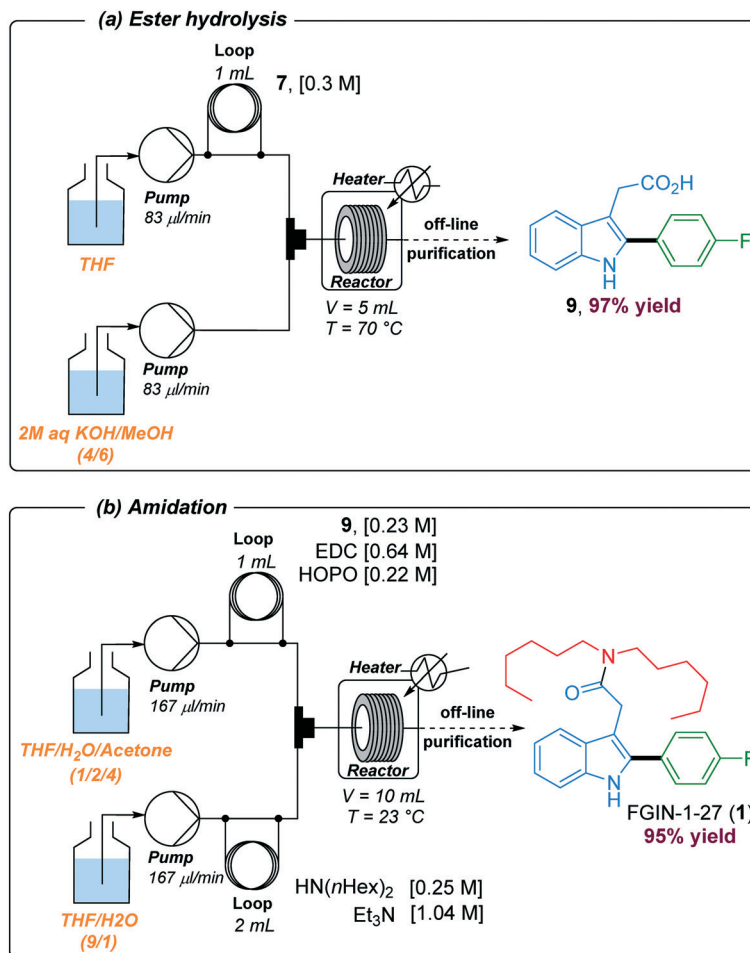
## Experimental section

### General information

All commercially available chemicals were used as received unless otherwise noted. High-field <sup>1</sup>H and <sup>13</sup>C NMR spectra were recorded at 300 or 400 and 75 or 100 MHz, respectively. <sup>1</sup>H and <sup>13</sup>C NMR spectra were referenced to the residual signal of the internal deuterated solvent (CDCl<sub>3</sub>) at 7.26 and 77.16 ppm, respectively, and coupling constants were measured in hertz. <sup>19</sup>F spectra were recorded at 40.88 MHz with a 1 T-benchtop spectrometer (Spinsolve, Magritek) equipped with a flow cell (4 mm id). The following abbreviations were used to explain the multiplicities: s = singlet, d = doublet, t = triplet, q = quartet, m = multiplet, and br = broad. FT-IR spectra were recorded in ATR mode. Wavelengths of maximum absorbance ( $\nu_{\text{max}}$ ) are quoted in wave number ( $\text{cm}^{-1}$ ). Flash column chromatography was performed using silica gel 60 (40–63  $\mu\text{m}$ ). In order to remove any trace of waste (Pd particles, inorganic salts...) which progressively deposits on the wall of the reactor coil, the tubing was washed every 100 hours of use with an aqueous solution of nitric acid (1 M, 50 mL), followed by thorough washing with water (100 mL) and CH<sub>3</sub>CN (100 mL).

### Details of the experimental flow setup

HPLC pumps (JASCO PU4185) were employed to flow the solution through the system. The reaction yields were determined by HPLC using the following conditions: Agela Promosil C18 column (3.5 mm × 150 mm, 5  $\mu\text{m}$ ), solvent: MeOH/H<sub>2</sub>O (70/30), isocratic mode, flow rate 0.5 mL  $\text{min}^{-1}$ , UV detection (254 nm).



Scheme 3 Reaction setups used for preparing acid 9 and FGIN-1-27 (1).

### 1*H*-Indole-3-acetic acid ethyl ester 6

Note that 1*H*-indole-3-acetic acid ethyl ester 6 is commercially available but it can be prepared as well from the corresponding acid by esterification following a modified published procedure.<sup>48</sup> Indole acetic acid (10 g, 57.14 mmol) was dissolved in dry EtOH (125 mL) in a 250 mL round bottom flask fitted with a reflux condenser and a calcium chloride guard tube. Sulfuric acid (10 mL, 0.19 mol) was added dropwise at 0 °C for 15 min and the resulting mixture was refluxed for 16 h at 75 °C. The volume of the reaction mixture was reduced to *ca.* 1/6 of its initial volume under vacuum and diluted with cold water (25 mL). The aqueous layer was extracted with EtOAc (5 × 50 mL). The combined organic layers were successively washed with H<sub>2</sub>O (25 mL), saturated NaHCO<sub>3</sub> solution (2 × 25 mL), H<sub>2</sub>O (2 × 25 mL) and saturated NaCl solution (2 × 25 mL). The organic phase was dried over MgSO<sub>4</sub> and concentrated under reduced pressure to give 6 (10.6 g, 91%) as a pale yellow solid which was used in the next step without further purification. mp 40 °C [Lit.<sup>49</sup> 42–45 °C]. IR (ATR)  $\nu$  3353, 2984, 1719, 1456, 1335, 1239, 1172, 1026, 735, 665, 598, 565. <sup>1</sup>H NMR (CDCl<sub>3</sub>, 300 MHz)  $\delta$  8.12 (br s), 7.64 (dm, 1H, *J* = 7.7 Hz), 7.34 (dm, 1H, *J* = 7.8

Hz), 7.21 (app dt, 1H, *J* = 1.3, 7.0 Hz), 7.17–7.13 (m, 2H), 4.18 (q, 2H, *J* = 7.1 Hz), 3.79 (s, 2H), 1.28 (t, 3H, *J* = 7.1 Hz). <sup>13</sup>C NMR (CDCl<sub>3</sub>, 75 MHz),  $\delta$  172.3, 136.2, 127.3, 123.2, 122.3, 119.7, 119.0, 111.3, 108.6, 60.9, 31.5, 14.4. HRMS (ESI+) *m/z* [M + Na]<sup>+</sup> calcd for C<sub>12</sub>H<sub>13</sub>NO<sub>2</sub>Na 226.0844; found: 226.0847.

### General experimental setup for the synthesis of 4-fluorobenzene diazonium tosylate 2

The experimental setup consisted of two streams as depicted in Scheme 1. The two inlets were equipped with PEEK injection loops (0.5 mL, 0.76 mm id). The first loop was loaded with 4-fluoroaniline 2 (0.2 M), PTSA (0.22 M) and C<sub>6</sub>F<sub>6</sub> (0.2 M) in MeOH, while the second loop was filled with a solution of *t*-BuONO (0.3 M) in MeOH. The two streams were merged in a PEEK T-shaped piece (internal volume: 11.4  $\mu\text{L}$ ) and the resulting mixture flowed in a PEEK coil reactor (5 mL, 0.76 mm id, 30 °C) at a flow rate of 0.5 mL min<sup>-1</sup>. The outlet of the reactor was connected to the flow cell of a benchtop NMR spectrometer. The NMR conversion was determined through 1D <sup>19</sup>F experiments at 40.88 MHz in stop-flow mode. A preparative experiment, without an in-line NMR spectrometer, was conducted with 5 mL sample loops

and 4-fluorobenzene diazonium tosylate **2** was isolated by precipitation in Et<sub>2</sub>O as a pale yellow solid (99 mg, 89%). mp 131 °C. IR (ATR)  $\nu$  3050, 2296, 1576, 1475, 1216, 1189, 1032, 1008, 848, 679, 564, 523 cm<sup>-1</sup>. <sup>1</sup>H NMR (MeOD, 400 MHz)  $\delta$  8.77–8.72 (m, 2H), 7.76–7.70 (m, 2H), 7.67 (d, 2H, *J* = 8.2 Hz), 7.22 (d, 2H, *J* = 7.9 Hz), 2.36 (s, 3H). <sup>19</sup>F NMR (MeOD, 376 MHz)  $\delta$  -86.4.

### General experimental setup for the optimization of indole 7

The experimental setup consisted of two streams as depicted in Scheme 2. The first stream, equipped with a stainless steel injection loop (0.5 mL, 0.76 mm id) loaded with a solution of indole **6** (0.1 M), Pd(OAc)<sub>2</sub> (see Table S1†) and naphthalene (0.1 M) in DMF/EtOAc (1/4), met in a stainless steel T-shaped piece (internal volume: 0.57  $\mu$ L) the second stream consisting of a solution of arenediazonium tosylate **2** in MeOH (0.1 M) loaded in the second stainless steel injection loop (2 mL, 1 mm id). The merged streams entered a stainless steel reactor coil (5 mL, 1 mm id) at the required flow rate (see Table S1†) and the resulting indole **7** was collected in vials and analyzed by HPLC to determine the reaction yield. An analytical sample of ethyl 2-(2-(*p*-tolyl)-1*H*-indol-3-yl)acetate **7** was obtained under the experimental conditions of experiment 18 after purification by flash chromatography (10% AcOEt–petroleum ether) as a white solid (58 mg, 78%). mp 109 °C. IR (ATR)  $\nu$  3354, 2988, 1711, 1453, 1438, 1314, 1270, 1221, 1178, 1034, 840, 744, 566 cm<sup>-1</sup>. <sup>1</sup>H NMR (CDCl<sub>3</sub>, 300 MHz)  $\delta$  8.15 (br s, 1H), 7.70–7.61 (m, 3H), 7.35 (d, 1H, *J* = 7.5 Hz), 7.25–7.14 (m, 4H), 4.18 (q, 2H, *J* = 7.2 Hz), 3.80 (s, 2H), 1.27 (t, 3H, *J* = 7.2 Hz). <sup>13</sup>C NMR (CDCl<sub>3</sub>, 75 MHz)  $\delta$  172.4, 164.4, 161.1, 135.8, 135.4, 130.2, 130.1, 129.0, 128.6, 128.6, 122.8, 120.2, 119.4, 116.2, 115.9, 111.0, 61.1, 31.2, 14.4. HRMS (ESI+) *m/z* [M + H]<sup>+</sup> calcd for C<sub>18</sub>H<sub>17</sub>O<sub>2</sub>NF 298.1243; found 298.1255.

### 2-(4-Fluorophenyl)-1*H*-indole-3-acetic acid **9**

The experimental setup consisted of two streams as depicted in Scheme 3a. In the first stream, a solution of indole **7** (0.3 M) in THF was loaded in an injection loop (1 mL, 0.76 mm id) while a solution of 2 M aqueous KOH in MeOH (4/6) was continuously pumped in the second stream. Both streams, each flowing at 83  $\mu$ L min<sup>-1</sup>, met in a stainless steel T-shaped piece (internal volume: 0.57  $\mu$ L) and reacted in a stainless steel reactor coil (5 mL, 1 mm id) at a flow rate of 166  $\mu$ L min<sup>-1</sup> (30 min residence time). The resulting acid **9** was collected in vials and neutralized with 2.5 M aqueous H<sub>3</sub>PO<sub>4</sub>. The biphasic mixture was extracted three times with Et<sub>2</sub>O, washed with brine, dried over MgSO<sub>4</sub> and concentrated under reduced pressure. The crude mixture was purified by flash chromatography (20% AcOEt – 80% cyclohexane) to give acid **9** as a white solid (79 mg, 97%). mp 179 °C. IR (ATR)  $\nu$  3424, 1698, 1500, 1432, 1311, 1217, 1184, 1155, 934, 839, 757, 623, 469 cm<sup>-1</sup>. <sup>1</sup>H NMR (MeOD, 300 MHz)  $\delta$  10.74 (br s, 1H), 7.74–7.68 (m, 2H), 7.57 (dd, 1H, *J* = 0.8, 7.9 Hz), 7.37 (app dt, 1H, *J* = 0.8, 8.0 Hz), 7.25–7.20 (m, 2H), 7.16–7.11 (m, 1H), 7.07–7.02 (m, 1H), 3.78 (s, 2H). <sup>13</sup>C NMR (MeOD, 75 MHz)  $\delta$  176.4,

163.8 (d, 1C, <sup>1</sup>*J*<sub>CF</sub> = 244 Hz), 137.6, 136.5, 131.2 (d, 2C, <sup>3</sup>*J*<sub>CF</sub> = 7.5 Hz), 130.5, 130.5, 130.2, 123.0, 120.3, 119.7, 116.5 (d, 2C, <sup>2</sup>*J*<sub>CF</sub> = 21 Hz), 112.0, 106.1, 31.5. HRMS (ESI-) *m/z* [M - H]<sup>-</sup> calcd for C<sub>16</sub>H<sub>11</sub>NO<sub>2</sub>F 268.0774; found: 268.0774.

### FGIN-1-27 (**1**)

The experimental setup consisted of two streams as depicted in Scheme 3b. In the first stream, an injection loop (1 mL, 0.76 mm id) was loaded with a solution of acid **9** (0.23 M), EDC·HCl (0.64 M) and HOPO (0.22 M) in a mixture of THF/H<sub>2</sub>O/acetone (1/2/4) while in the second stream, a 2 mL injection loop (0.76 mm id) was loaded with a solution of dihexylamine (0.25 M) and Et<sub>3</sub>N (1.04 M) in a mixture of THF/H<sub>2</sub>O (9/1). Both streams, flowing at 167  $\mu$ L min<sup>-1</sup>, met in a T-shaped piece (internal volume: 0.57  $\mu$ L) and reacted at 23 °C in a stainless steel coil reactor (10 mL, 1 mm id) for a total of 30 min of residence time. The resulting collected mixture was diluted with water (10 mL) and washed three times with dichloromethane (3  $\times$  10 mL). The collected organic extracts were washed with brine (15 mL), dried over MgSO<sub>4</sub>, filtered and concentrated under reduced pressure. The crude mixture was purified by flash chromatography (8% AcOEt–cyclohexane to 15% AcOEt–cyclohexane) to give FGIN-1-27 (**1**) as a white solid (93 mg, 95%). mp 97 °C. IR (ATR)  $\nu$  3213, 2927, 2854, 1618, 1497, 1451, 1371, 1342, 1226, 1155, 1011, 836, 744, 563 cm<sup>-1</sup>. <sup>1</sup>H NMR (CDCl<sub>3</sub>, 300 MHz)  $\delta$  8.27 (s, 1H), 7.65 (d, 1H, *J* = 7.6 Hz), 7.54–7.48 (m, 2H), 7.29–7.27 (m, 1H), 7.18–7.07 (m, 4H), 3.84 (s, 2H), 3.30 (t, 2H, *J* = 7.5 Hz), 3.13 (t, 2H, *J* = 7.9 Hz), 1.51–1.35 (m, 4H), 1.26–1.10 (m, 10H), 1.06–0.97 (m, 2H), 0.88–0.83 (m, 6H). <sup>13</sup>C NMR (CDCl<sub>3</sub>, 75 MHz)  $\delta$  170.7, 162.6 (d, 1C, <sup>1</sup>*J*<sub>CF</sub> = 246 Hz), 136.1, 134.7, 130.2 (d, 2C, <sup>3</sup>*J*<sub>CF</sub> = 7.5 Hz), 129.1, 129.0 (d, 2C, <sup>4</sup>*J*<sub>CF</sub> = 3.8 Hz), 122.6, 120.1, 119.6, 116.0 (d, 2C, <sup>2</sup>*J*<sub>CF</sub> = 21.8 Hz), 110.9, 107.3, 48.4, 46.4, 31.8, 31.6, 31.0, 29.2, 27.8, 26.8, 26.6, 22.7, 22.7, 14.2, 14.1. HRMS (ASAP+) *m/z* [M + H]<sup>+</sup> calcd for C<sub>28</sub>H<sub>38</sub>N<sub>2</sub>O<sub>2</sub>F 437.2968; found: 437.2961.

## Conclusion

In summary, we developed a full flow synthesis of translocator protein ligand FGIN-1-27 (**1**) in 4 steps and with a 64% overall yield from inexpensive and commercially available starting materials using the palladium-catalyzed direct C–H arylation of 1*H*-indole-3-acetic acid ethyl ester **6** with 4-fluorobenzene diazonium tosylate **2** as the key step. We also demonstrated the power of flow reactors integrating an in-line benchtop NMR spectrometer to accurately monitor in quasi real-time the reaction progress in optimization stages. For instance, the formation of 4-fluorobenzene diazonium tosylate **2** through the diazotization of the corresponding aniline **3** was unusually and advantageously followed by <sup>19</sup>F NMR experiments which addressed the signal overlap issues observed with more traditional <sup>1</sup>H NMR analysis. For the more complex multi-dimensional optimization of the direct C–H arylation of 1*H*-indole-3-acetic acid ethyl ester **6** with 4-fluorobenzene diazonium tosylate **2**, the use of a feedback optimization



algorithm, assisting chemists in the decision-making process, minimized the number of experiments required to locate an optimum in a short time frame. Through this contribution, we demonstrated that process analytical technologies and optimization algorithms are powerful tools to improve processing times, safety and reaction yields.

## Author contributions

FXF conceived the project and coordinated the efforts of the research team. NV designed the initial route for FGIN-1-27 and conducted NMR experiments. ECA and EB conducted chemical experiments in flow. EW and DCB developed the optimization algorithm. PG and JF supervised the NMR experiments. MRZ supervised the chemical experiments. FXF wrote the paper with input from all authors.

## Conflicts of interest

There are no conflicts to declare.

## Acknowledgements

We gratefully acknowledge the University of Nantes, the “Centre National de la Recherche Scientifique” (CNRS) and the “Région des Pays de la Loire” in the framework of the SmartCat project for financial support. N. Vasudevan thanks the UBL for a grant. The assistance of Dr. Shrikant Kunjir (CEISAM, University of Nantes) for the recording of  $^{19}\text{F}$  NMR spectra is greatly appreciated. Mr. Romain De Luca (University of Nantes) is gratefully acknowledged for preliminary experiments. We acknowledge Julie Hémez (CEISAM, University of Nantes) for HRMS analyses.

## References

- 1 E. Romeo, J. Auta, A. P. Kozikowski, D. Ma, V. Papadopoulos, G. Puia, E. Costa and A. Guidotti, *J. Pharmacol. Exp. Ther.*, 1992, **262**, 971–978.
- 2 E. Romeo, S. Cavallaro, A. Korneyev, A. P. Kozikowski, D. Ma, A. Polo, E. Costa and A. Guidotti, *J. Pharmacol. Exp. Ther.*, 1993, **267**, 462–471.
- 3 M. G. Lima-Maximino, J. Cueto-Escobedo, J. F. Rodríguez-Landa and C. Maximino, *Pharmacol., Biochem. Behav.*, 2018, **171**, 66–73.
- 4 S. M. Petralia and C. A. Frye, *Psychopharmacology*, 2005, **178**, 174–182.
- 5 J. Lv, S. Jiang, Y. Yang, X. Zhang, R. Gao, Y. Cao and G. Song, *Front. Pharmacol.*, 2020, **11**, 602889.
- 6 A. Singh, M. Dashnyam, B. Chim, T. M. Escobar, A. E. Dulcey, X. Hu, K. M. Wilson, P. P. Koganti, C. A. Spinner, X. Xu, A. Jadhav, N. Southall, J. Marugan, V. Selvaraj, V. Lazarevic, S. A. Muljo and M. Ferrer, *Sci. Rep.*, 2020, **10**, 3766.
- 7 A. P. Kozikowski, D. Ma, E. Romeo, J. Auta, V. Papadopoulos, G. Puia, E. Costa and A. Guidotti, *Angew. Chem., Int. Ed. Engl.*, 1992, **31**, 1060–1062.
- 8 T. Opatz and D. Ferenc, *Org. Lett.*, 2006, **8**, 4473–4475.
- 9 M. B. Plutschack, B. Pieber, K. Gilmore and P. H. Seeberger, *Chem. Rev.*, 2017, **117**, 11796–11893.
- 10 R. Gérardy, N. Emmanuel, T. Toupy, V.-E. Kassin, N. N. Tshibalonza, M. Schmitz and J.-C. M. Monbaliu, *Eur. J. Org. Chem.*, 2018, **2018**, 2301–2351.
- 11 V. Hessel, D. Kralisch, N. Kockmann, T. Noël and Q. Wang, *ChemSusChem*, 2013, **6**, 746–789.
- 12 B. J. Deadman, S. G. Collins and A. R. Maguire, *Chem. – Eur. J.*, 2015, **21**, 2298–2308.
- 13 N. Oger, E. Le Grogneq and F.-X. Felpin, *Org. Chem. Front.*, 2015, **2**, 590–614.
- 14 M. Movsisyan, E. I. P. Delbeke, J. K. E. T. Berton, C. Battilocchio, S. V. Ley and C. V. Stevens, *Chem. Soc. Rev.*, 2016, **45**, 4892–4928.
- 15 B. Gutmann and O. C. Kappe, *J. Flow Chem.*, 2017, **7**, 65–71.
- 16 N. Oger, M. d'Halluin, E. Le Grogneq and F.-X. Felpin, *Org. Process Res. Dev.*, 2014, **18**, 1786–1801.
- 17 N. Vasudevan, E. Wimmer, E. Barré, D. Cortés-Borda, M. Rodríguez-Zubiri and F.-X. Felpin, *Adv. Synth. Catal.*, 2021, **363**, 791–799.
- 18 N. Oger, E. Le Grogneq and F.-X. Felpin, *J. Org. Chem.*, 2014, **79**, 8255–8262.
- 19 V. Sans, L. Porwol, V. Dragone and L. Cronin, *Chem. Sci.*, 2015, **6**, 1258–1264.
- 20 B. Picard, B. Gouilleux, T. Lebleu, J. Maddaluno, I. Chataigner, M. Penhoat, F.-X. Felpin, P. Giraudeau and J. Legros, *Angew. Chem., Int. Ed.*, 2017, **56**, 7568–7572.
- 21 B. Ahmed-Omer, E. Sliwinski, J. P. Cerroti and S. V. Ley, *Org. Process Res. Dev.*, 2016, **20**, 1603–1614.
- 22 P. Giraudeau and F.-X. Felpin, *React. Chem. Eng.*, 2018, **3**, 399–413.
- 23 T. H. Rehm, C. Hofmann, D. Reinhard, H.-J. Kost, P. Lob, M. Besold, K. Welzel, J. Barten, A. Didenko, D. V. Sevenard, B. Lix, A. R. Hillson and S. D. Riegel, *React. Chem. Eng.*, 2017, **2**, 315–323.
- 24 B. Musio, E. Gala and S. V. Ley, *ACS Sustainable Chem. Eng.*, 2018, **6**, 1489–1495.
- 25 I. K. Barben and H. Suschitzky, *J. Chem. Soc.*, 1960, 2735–2739.
- 26 R. Khan, S. Boonseng, P. D. Kemmitt, R. Felix, S. J. Coles, G. J. Tizzard, G. Williams, O. Simmonds, J.-L. Harvey, J. Atack, H. Cox and J. Spencer, *Adv. Synth. Catal.*, 2017, **359**, 3261–3269.
- 27 O. Fischer and M. R. Heinrich, *Chem. – Eur. J.*, 2021, **27**, 5417–5421.
- 28 A. Krause, E. Sperlich and B. Schmidt, *Org. Biomol. Chem.*, 2021, **19**, 4292–4302.
- 29 M. P. Doyle and W. J. Bryker, *J. Org. Chem.*, 1979, **44**, 1572–1574.
- 30 K. S. Nalivela, M. Tilley, M. A. McGuire and M. G. Organ, *Chem. – Eur. J.*, 2014, **20**, 6603–6607.
- 31 J. P. McMullen, M. T. Stone, S. L. Buchwald and K. F. Jensen, *Angew. Chem., Int. Ed.*, 2010, **49**, 7076–7080.
- 32 R. A. Bourne, R. A. Skilton, A. J. Parrott, D. J. Irvine and M. Poliakov, *Org. Process Res. Dev.*, 2011, **15**, 932–938.
- 33 D. N. Jumbam, R. A. Skilton, A. J. Parrott, R. A. Bourne and M. Poliakov, *J. Flow Chem.*, 2012, **2**, 24–27.

- 34 Z. Amara, E. S. Streng, R. A. Skilton, J. Jin, M. W. George and M. Poliakoff, *Eur. J. Org. Chem.*, 2015, 6141–6145.
- 35 D. E. Fitzpatrick, C. Battilocchio and S. V. Ley, *Org. Process Res. Dev.*, 2016, **20**, 386–394.
- 36 K. Poscharny, D. C. Fabry, S. Heddrich, E. Sugiono, M. A. Liauw and M. Rueping, *Tetrahedron*, 2018, **74**, 3171–3175.
- 37 H.-W. Hsieh, C. W. Coley, L. M. Baumgartner, K. F. Jensen and R. I. Robinson, *Org. Process Res. Dev.*, 2018, **22**, 542–550.
- 38 E. Wimmer, D. Cortés-Borda, S. Brochard, E. Barré, C. Truchet and F.-X. Felpin, *React. Chem. Eng.*, 2019, **4**, 1608–1615.
- 39 D. Cortés-Borda, E. Wimmer, B. Gouilleux, E. Barré, N. Oger, L. Goulamaly, L. Peault, B. Charrier, C. Truchet, P. Giraudeau, M. Rodriguez-Zubiri, E. Le Grogneec and F.-X. Felpin, *J. Org. Chem.*, 2018, **83**, 14286–14299.
- 40 E. C. Aka, E. Wimmer, E. Barré, N. Vasudevan, D. Cortés-Borda, T. Ekou, L. Ekou, M. Rodriguez-Zubiri and F.-X. Felpin, *J. Org. Chem.*, 2019, **84**, 14101–14112.
- 41 D. Cortés-Borda, K. V. Kutonova, C. Jamet, M. E. Trusova, F. Zammattio, C. Truchet, M. Rodriguez-Zubiri and F.-X. Felpin, *Org. Process Res. Dev.*, 2016, **20**, 1979–1987.
- 42 D. G. Brown and J. Boström, *J. Med. Chem.*, 2016, **59**, 4443–4458.
- 43 F. Albericio and A. El-Faham, *Org. Process Res. Dev.*, 2018, **22**, 760–772.
- 44 T. D. White, K. D. Berglund, J. M. Groh, M. D. Johnson, R. D. Miller and M. H. Yates, *Org. Process Res. Dev.*, 2012, **16**, 939–957.
- 45 C. S. Polster, K. P. Cole, C. L. Burcham, B. M. Campbell, A. L. Frederick, M. M. Hansen, M. Harding, M. R. Heller, M. T. Miller, J. L. Phillips, P. M. Pollock and N. Zaborenko, *Org. Process Res. Dev.*, 2014, **18**, 1295–1309.
- 46 B. Li, G. A. Weisenburger and J. C. McWilliams, *Org. Process Res. Dev.*, 2020, **24**, 2311–2318.
- 47 J. B. Sperry, C. J. Minter, J. Tao, R. Johnson, R. Duzguner, M. Hawksworth, S. Oke, P. F. Richardson, R. Barnhart, D. R. Bill, R. A. Giusto and J. D. Weaver, *Org. Process Res. Dev.*, 2018, **22**, 1262–1275.
- 48 D. Kumar, N. M. Kumar, B. Noel and K. Shah, *Eur. J. Med. Chem.*, 2012, **55**, 432–438.
- 49 C. M. Griffiths-Jones and D. W. Knight, *Tetrahedron*, 2011, **67**, 8515–8528.